

# Unidirectional weak visibility in band gap region of one dimensional parity-time-symmetric photonic crystal

Tiecheng Wang\*

*College of Physics and Electronic Engineering, Shanxi University, 030006, Taiyuan, China*

(Dated: December 22, 2024)

We explore the absorption and scattering properties of one dimensional parity-time ( $\mathcal{PT}$ )-symmetric photonic crystal. In addition to the familiar transmittance and reflectance, we give the definition of the generalized absorptance to include the amplifying effect of the dielectric with negative imaginary part of the permittivity, moreover, we present the mathematical expressions of the transmittance, reflectances and absorptances from both sides of this photonic crystal with  $N$  periods in terms of the elements of the transfer matrix of the primitive cell. The complex band structure of this photonic crystal is studied and the corresponding evolutions of the exceptional points,  $\mathcal{PT}$ -exact phase and  $\mathcal{PT}$ -broken phase are disclosed. Near the exceptional points, we find some singular behaviors, the transmittance and reflectances from both sides are all greater than one and even all reach large values at the same time, then the corresponding absorptances from both sides are negative. In the band gap, the transmittance is zero, the reflectance from one side can be very large, while the reflectance from the other side is very small, we call this phenomenon unidirectional weak visibility. We believe that these phenomena are very beneficial for the design of the optical devices.

## I. INTRODUCTION

In recent years, parity-time- ( $\mathcal{PT}$ )-symmetric photonic systems have attracted keen research interest [1]. This is motivated by the study of non-Hermitian quantum mechanics [2–5], the non-Hermitian Hamiltonian is  $\mathcal{PT}$ -symmetric when the complex potential satisfies  $V^*(-x) = V(x)$ . If the eigenstate is also  $\mathcal{PT}$ -symmetric, the eigenvalue is real and the system is in a  $\mathcal{PT}$ -exact phase, otherwise the eigenstate isn't  $\mathcal{PT}$ -symmetric, two complex eigenvalues which are conjugate to each other arise and the system is in a  $\mathcal{PT}$ -broken phase. In optics,  $\mathcal{PT}$ -symmetric systems are characterized by the complex index of refraction with balanced gain and loss  $n^*(-x) = n(x)$ , like the situation in quantum mechanics,  $\mathcal{PT}$ -symmetric photonic systems have different phases and go through a phase transition from a  $\mathcal{PT}$ -exact phase to a  $\mathcal{PT}$ -broken phase at an exceptional point [6–10].

$\mathcal{PT}$ -symmetric photonic systems also exhibit other various intriguing regularities and phenomena. Unidirectional invisibility is a typical optical effect, it is found that the interplay of Bragg scattering and  $\mathcal{PT}$ -symmetry allows for unidirectional invisibility in a wide range of frequencies around the Bragg point [11–15], the nonlinear optical structures also support unidirectional invisibility [16]. The idea of a  $\mathcal{PT}$ -symmetric coherent perfect absorber (CPA) laser is proposed and a  $\mathcal{PT}$ -symmetric optical medium can act simultaneously as a laser oscillator and as a CPA [17–20]. Through the scattering matrix formalism, the existence of a transition between  $\mathcal{PT}$ -exact scattering eigenstates and  $\mathcal{PT}$ -broken scattering eigenstate has been disclosed [21], the product of the two eigenvalues of the scattering matrix is one out of the

optical reciprocity, in a  $\mathcal{PT}$ -exact phase, both eigenvalues are unimodular, while in a  $\mathcal{PT}$ -broken phase this condition can't be satisfied [22].  $\mathcal{PT}$ -symmetric photonic systems violate the normal photon flux conservation but obey the generalized unitarity relations, these relations illustrate the existence of anisotropic transmission resonances (ATRs) [23]. Direction-dependent  $\mathcal{PT}$ -phase transition is found in a dielectric waveguide structure, in the forward direction, this transition is thresholdless, whereas in the backward direction it has nonzero threshold [24–27]. We focus on  $\mathcal{PT}$ -symmetric photonic crystal, the complex band structure of the one dimensional  $\mathcal{PT}$ -symmetric photonic crystal (1DPTSPC) is calculated and analyzed, as the non-Hermiticity increases two types of  $\mathcal{PT}$ -phase diagrams are found [28, 29]. The exceptional contours and band structure in the two dimensional  $\mathcal{PT}$ -symmetric photonic crystal are also studied, whose non-Hermitian primitive cell is an integer multiple of the primitive cell of the underlying Hermitian system [30].

Based on the previous investigations, in this paper, we study the transmission, reflection, absorption and emission properties of 1DPTSPC. So far, the transfer matrix method and the scattering matrix method have been proposed to define a  $\mathcal{PT}$ -exact phase and a  $\mathcal{PT}$ -broken phase for the  $\mathcal{PT}$ -symmetric photonic systems, however, these two methods provide different definitions. The transfer matrix method is more physical meaningful for the  $\mathcal{PT}$ -symmetric photonic crystal according to Bloch theorem. We provide a systematic study of the scattering properties as the non-Hermiticity increases, special properties emerge around the exceptional points. Moreover, the transfer matrix method is approved for the  $\mathcal{PT}$ -symmetric photonic crystal which can be also seen from the aspect of its optical properties. This paper is organized as follows, in Section II, we present our theoretical model, define the general absorptance and derive

\* Corresponding author: tcwang@sxu.edu.cn

the mathematical expressions of the optical properties of 1DPTSPC. In Section III, we analyze these optical properties combining with the complex and real band structures. We conclude with a summary in Section IV.

## II. MODEL AND FORMULATION

Before we study the transmittance, reflectances and absorptances of 1DPTSPC, it is worth reviewing the properties of the general  $\mathcal{PT}$ -symmetric photonic structure to introduce our research. Its transfer matrix  $M(\omega)$  which connects the waves at two sides (see an example Fig. 1) is referred to by many researchers [31, 32]

$$\begin{pmatrix} C \\ D \end{pmatrix} = \begin{pmatrix} M_{11}(\omega) & M_{12}(\omega) \\ M_{21}(\omega) & M_{22}(\omega) \end{pmatrix} \begin{pmatrix} A \\ B \end{pmatrix}. \quad (1)$$

Following from the theoretical analysis from the Ref. [17], the components of the transfer matrix  $M(\omega)$  fulfill the relations  $M_{22}(\omega) = M_{11}^*(\omega^*)$ ,  $M_{12}(\omega) = -M_{12}^*(\omega^*)$  and  $M_{21}(\omega) = -M_{21}^*(\omega^*)$ . If the angular frequency  $\omega$  is real, the transfer matrix can be parametrized as

$$M(\omega) = \begin{pmatrix} a^* & ic \\ -ib & a \end{pmatrix}, \quad (2)$$

where the parameter  $a$  is complex while  $b$  and  $c$  are real, they are related to each other by the condition  $|a|^2 - bc = 1$ . The scattering matrix  $S(\omega)$  [22, 23] can be obtained by transforming the transfer matrix  $M(\omega)$  into the form

$$\begin{pmatrix} B \\ C \end{pmatrix} = S(\omega) \begin{pmatrix} A \\ D \end{pmatrix} \equiv \begin{pmatrix} r_L & t \\ t & r_R \end{pmatrix} \begin{pmatrix} A \\ D \end{pmatrix}, \quad (3)$$

here  $t \equiv t_L = t_R = \frac{1}{a}$ ,  $r_L = \frac{ib}{a}$  and  $r_R = \frac{ic}{a}$  represent the transmission, reflection coefficients from the left and right sides. On the basis of the relation between those parameters, the generalized conservation law  $|T - 1| = \sqrt{R_L R_R}$  can be derived for the transmittance  $T = |t|^2$  and reflectances  $R_L = |r_L|^2$ ,  $R_R = |r_R|^2$  from the left and right sides. If the photonic structure satisfies only parity symmetry,  $M_{21}(\omega) = -M_{12}(\omega)$  can be derived, or if the photonic structure possesses only time reversal symmetry,  $M_{22}(\omega) = M_{11}^*(\omega^*)$  and  $M_{21}(\omega) = M_{12}^*(\omega^*)$  can be obtained as well. Consequently, for real angular frequency the reflectances from the left and right sides are equal to each other  $R_L = R_R$  for these two situations. As a comparison, for real angular frequency the relation  $R_L \neq R_R$  holds in general for  $\mathcal{PT}$ -symmetric system. In some special cases, the transmittance is unity, the reflectance from one side is zero and the reflectance from the other side is nonzero, this phenomenon is known as ATRs.

The spontaneous symmetric breaking of this scattering matrix  $S(\omega)$  has been studied [23]. The eigenvalues of this scattering matrix is found as

$$\lambda_1, \lambda_2 = \frac{r_L + r_R \pm \sqrt{(r_L - r_R)^2 + 4t^2}}{2}. \quad (4)$$

A criterion for the phase boundary is derived from the degeneracy of these two eigenvalues, the system is in a  $\mathcal{PT}$ -exact phase when  $\frac{R_L + R_R}{2} - T < 1$ , and in this phase  $|\lambda_1| = |\lambda_2| = 1$ , while the system is in a  $\mathcal{PT}$ -broken phase when  $\frac{R_L + R_R}{2} - T > 1$ , and in this phase  $|\lambda_1| = 1/|\lambda_2| \neq 1$ ,  $\frac{R_L + R_R}{2} - T = 1$  is the phase transition boundary which corresponds to the exceptional points. In addition to this  $S(\omega)$  matrix, there is another optional definition for the scattering matrix  $S_c(\omega)$  defined as

$$\begin{pmatrix} C \\ B \end{pmatrix} = S_c(\omega) \begin{pmatrix} A \\ D \end{pmatrix} \equiv \begin{pmatrix} t & r_R \\ r_L & t \end{pmatrix} \begin{pmatrix} A \\ D \end{pmatrix}. \quad (5)$$

Actually  $S_c(\omega)$  is related to  $S(\omega)$  by the permutation of the scattered waves. The eigenvalues of the scattering matrix are changed after this permutation operation

$$\lambda_{c1}, \lambda_{c2} = t \pm \sqrt{r_R r_L}. \quad (6)$$

The criterion for the phase boundary in this case is located at  $T = 1$ , if  $T < 1$ , the eigenvalues are real and  $|\lambda_{c1}| = |\lambda_{c2}| = 1$ , and the system is in the  $\mathcal{PT}$ -exact phase, if  $T > 1$ , the eigenvalues are complex and  $|\lambda_{c1}| = 1/|\lambda_{c2}| \neq 1$ , while the system is in the  $\mathcal{PT}$ -broken phase,  $T = 1$  is the phase transition boundary which corresponds to the exceptional points. The first scattering matrix  $S(\omega)$  is supposed to be physically meaningful because the energy spectrum expressed as complex frequencies of the corresponding effective Hamiltonian fits the eigenvalue spectrum of the  $S(\omega)$  matrix but not the eigenvalue spectrum of the  $S_c(\omega)$  matrix [23].

In our work, through the investigation about the  $\mathcal{PT}$ -symmetric photonic crystal, we point out a different view from the above mentioned works that the study on the eigenvalues of the transfer matrix  $M(\omega)$  is more physically meaningful. This eigenvalue spectrum is closely related to the band structure, the complex band structure is already explored well by expressing the Bloch wave function of the  $\mathcal{PT}$ -symmetric system as linear superposition of the Bloch wave function of the corresponding optical system in the absence of loss and gain. We will expound why the spontaneous symmetric breaking presented by the eigenvalue of the transfer matrix is physically meaningful by exploring the optical scattering and absorption properties of 1DPTSPC.

In order to give a study on the optical properties of 1DPTSPC as comprehensively as possible, we also consider the absorption or emission of the  $\mathcal{PT}$ -symmetric structure, to start with, their definitions should be given correctly. Consider a general optical system, the energy flow densities of the light incident from its left and right sides are denoted by  $S_L^+$  and  $S_R^+$ , and that of the light emitted into the left and right sides are marked by  $S_L^-$  and  $S_R^-$ . If this system is made up of absorbing materials with positive imaginary permittivities, the absorptance can be defined as  $\frac{S_L^+ + S_R^+ - S_L^- - S_R^-}{S_L^+ + S_R^+}$ . On the other hand, if the imaginary permittivities are negative, the intensity of the light can be amplified, the amplified rate is given by

$\frac{S_L^- + S_R^- - S_L^+ - S_R^+}{S_L^+ + S_R^+}$ . Combining these two cases, if the system is composed of the absorbing or active materials or both of them, the generalized absorptance can be defined as

$$W = \frac{S_L^+ + S_R^+ - S_L^- - S_R^-}{S_L^+ + S_R^+}. \quad (7)$$

If  $W$  is greater than zero, the optical effect is absorptive, otherwise if  $W$  is less than zero the optical effect is amplifying. When  $W$  is equal to zero, the total energy flow density of the outgoing light is equal to that of the incoming light. In special cases, when the incoming light is only incident from the left side or the right side, the absorptances for these two cases can be expressed as

$$W_L = 1 - T - R_L, W_R = 1 - T - R_R. \quad (8)$$

By using the generalized conservation law, these absorptances can be expressed by the other reflectances

$$W_L = 1 - T - \frac{(1 - T)^2}{R_R}, W_R = 1 - T - \frac{(1 - T)^2}{R_L}. \quad (9)$$

They hold except the cases  $R_R = 0$  and  $R_L = 0$ , respectively. If  $R_R = 0$  or  $R_L = 0$ ,  $T = 0$ , therefore,  $W_L = -R_L$  or  $W_R = -R_R$ , correspondingly. We can also obtain the relation between  $W_L$  and  $W_R$  by using the generalized conservation law as well

$$W_L W_R + (T - 1)(W_L + W_R) = 0. \quad (10)$$

At the transmission resonances  $T = 1$  where the incoming lights are unidirectional reflected, the absorptances satisfy  $W_L W_R = 0$ , that means in this case the absorptance is zero from one side.

The primitive cell of the 1DPTSPC in our work is composed of four layers as shown in Fig. 1. Their relative permittivities which describe the balanced gain and loss are denoted by  $\epsilon'_\alpha - i\epsilon''_\alpha$ ,  $\epsilon'_\beta + i\epsilon''_\beta$ ,  $\epsilon'_\beta - i\epsilon''_\beta$  and  $\epsilon'_\alpha + i\epsilon''_\alpha$ , these parameters  $\epsilon'_{\alpha(\beta)}$  and  $\epsilon''_{\alpha(\beta)}$  are positive real number. In the remainder of this work, we choose  $\epsilon''_\alpha = \epsilon''_\beta = \epsilon''$  for the sake of simplicity, the real parts of these relative permittivities are fixed at  $\epsilon'_\alpha = 1.1$  and  $\epsilon'_\beta = 4.0$ , the thicknesses are taken as  $d_\alpha = 0.35\Lambda$  and  $d_\beta = 0.15\Lambda$ , where  $\Lambda$  is the thickness of a primitive cell, and we assume that Eq. (1) gives the transfer matrix for the primitive cell which is a special case of  $\mathcal{PT}$ -symmetric structure. Bloch theorem states the physical meaning fundamentally of the eigenvalue and eigenfunction of the transfer matrix

$$M(\omega) \begin{pmatrix} A \\ B \end{pmatrix} = e^{iK\Lambda} \begin{pmatrix} A \\ B \end{pmatrix}, \quad (11)$$

where both sides of the unit cell are filled with air. The complex band structure can be calculated by expressing a

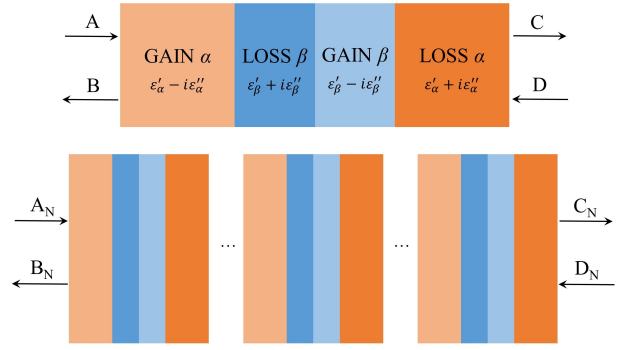


Figure 1. (Color online) Schematic picture of the 1DPTSPC, the top part shows the primitive cell made up of four layers with the relative permittivities  $\epsilon'_\alpha - i\epsilon''_\alpha$ ,  $\epsilon'_\beta + i\epsilon''_\beta$ ,  $\epsilon'_\beta - i\epsilon''_\beta$  and  $\epsilon'_\alpha + i\epsilon''_\alpha$ , the thicknesses are denoted by  $d_\alpha$  and  $d_\beta$ .

Bloch state of the  $\mathcal{PT}$ -symmetric system as linear superposition of the Bloch states of the corresponding optical system in the absence of loss and gain, then substitute it into Helmholtz equation, we can obtain the relation between the real wave vector  $K = K_c$  and complex eigenfrequency  $\omega = \omega_c = \omega_{cr} + i\omega_{ci}$ , in this criterion, if the imaginary part of this eigenfrequency  $\omega_{ci}$  is zero, the system is in a  $\mathcal{PT}$ -exact phase, otherwise if  $\omega_{ci}$  isn't zero, the system is in a  $\mathcal{PT}$ -broken phase, the transition boundary corresponds to the exceptional points. In the traditional transfer matrix method the band structure can be derived from  $\cos(K_a\Lambda) = (M_{11}(\omega) + M_{22}(\omega))/2$  by scanning the real frequency, the frequency is real  $\omega = \omega_a$  while the wave vector is complex  $K = K_a = K_{ar} + iK_{ai}$ , if the imaginary part of this wave vector  $K_{ai}$  is zero, the eigenstate is in a conduction band, otherwise if  $K_{ai}$  isn't zero, the eigenstate is in a forbidden band, we call this real band structure because the eigenfrequency here is real.

Now let us turn to the transmittance, reflectances from both air sides of the 1DPTSPC with  $N$  unit cells, the total transfer matrix for this model as shown in Fig. 1 is given by

$$\begin{pmatrix} C_N \\ D_N \end{pmatrix} = \begin{pmatrix} M_{11}(\omega) & M_{12}(\omega) \\ M_{21}(\omega) & M_{22}(\omega) \end{pmatrix}^N \begin{pmatrix} A_N \\ B_N \end{pmatrix}. \quad (12)$$

Here we assume that every unit cell is surrounded by infinite thin air films in both sides. The frequency is taken to be real because we focus on the scattering properties when the frequency of the light is real, therefore the transfer matrix can be taken as the form of Eq. (2). The  $N$ th power of a unimodular matrix  $M(\omega)$  can be simplified by the following matrix identity [31]

$$\begin{pmatrix} M_{11} & M_{12} \\ M_{21} & M_{22} \end{pmatrix}^N = \begin{pmatrix} M_{11}U_{N-1} - U_{N-2} & M_{12}U_{N-1} \\ M_{21}U_{N-1} & M_{22}U_{N-1} - U_{N-2} \end{pmatrix}, \quad (13)$$

here  $U_N = \frac{\sin(N+1)K_a\Lambda}{\sin K_a\Lambda}$ . Substituting Eq. (13) into Eq. (12) and using the parametrized form in Eq. (2),

we can obtain the transmission and reflection coefficients

$$t_N = \frac{1}{aU_{N-1} - U_{N-2}}, \quad (14a)$$

$$r_{NL} = \frac{ibU_{N-1}}{aU_{N-1} - U_{N-2}}, \quad r_{NR} = \frac{icU_{N-1}}{aU_{N-1} - U_{N-2}}. \quad (14b)$$

Furthermore, using the dispersion relation we have the corresponding transmittance  $T_N$ , reflectances  $R_{NL}$  and  $R_{NR}$ , and the absorptances  $W_{NL}$  and  $W_{NR}$

$$T_N \equiv |t_N|^2 = \frac{1}{bc \sin^2 NK_a \Lambda / \sin^2 K_a \Lambda + 1}, \quad (15a)$$

$$R_{NL} \equiv |r_{NL}|^2 = \frac{b^2}{bc + \sin^2 K_a \Lambda / \sin^2 NK_a \Lambda}, \quad (15b)$$

$$R_{NR} \equiv |r_{NR}|^2 = \frac{c^2}{bc + \sin^2 K_a \Lambda / \sin^2 NK_a \Lambda}, \quad (15c)$$

$$W_{NL} \equiv 1 - T - R_{NL} = \frac{bc - b^2}{bc + \sin^2 K_a \Lambda / \sin^2 NK_a \Lambda}, \quad (15d)$$

$$W_{NR} \equiv 1 - T - R_{NR} = \frac{bc - c^2}{bc + \sin^2 K_a \Lambda / \sin^2 NK_a \Lambda}. \quad (15e)$$

Because this photonic crystal is composed of  $N$   $\mathcal{PT}$ -symmetric unit cells, the generalized conservation law also holds for  $T_N$ ,  $R_{NL}$  and  $R_{NR}$ , and the phase relationships among the transmission and reflection also hold for  $t_N$ ,  $r_{NL}$  and  $r_{NR}$ , in another way, the basic generalized unitarity relation  $r_{NL}r_{NR} = t_N^2 \left(1 - \frac{1}{T_N}\right)$  can be proved by using the specific expressions of Eq. (14). At the frequency where  $\sin(NK_a \Lambda) = 0$  and  $\sin(K_a \Lambda) \neq 0$  are satisfied, from Eq. (15) we obtain

$$T_N = 1, R_{NL} = 0, R_{NR} = 0, W_{NL} = 0, W_{NR} = 0. \quad (16)$$

This case belongs to transmission resonances which isn't anisotropic.

In the above mentioned scattering properties, if the frequency is located at a conduction band,  $K_a$  is real number  $K_{ai} = 0$  and replaces  $K$  in Eqs. (13)-(15), on the other hand, if the frequency is located at the band gap,  $K_a \Lambda = m\pi + iK_{ai}\Lambda$  ( $m$  is an integer), and

$$T_N = \frac{1}{bc \sinh^2 NK_{ai}\Lambda / \sinh^2 K_{ai}\Lambda + 1}, \quad (17a)$$

$$R_{NL} = \frac{b^2}{bc + \sinh^2 K_{ai}\Lambda / \sinh^2 NK_{ai}\Lambda}, \quad (17b)$$

$$R_{NR} = \frac{c^2}{bc + \sinh^2 K_{ai}\Lambda / \sinh^2 NK_{ai}\Lambda}, \quad (17c)$$

$$W_{NL} = \frac{bc - b^2}{bc + \sinh^2 K_{ai}\Lambda / \sinh^2 NK_{ai}\Lambda}, \quad (17d)$$

$$W_{NR} = \frac{bc - c^2}{bc + \sinh^2 K_{ai}\Lambda / \sinh^2 NK_{ai}\Lambda}. \quad (17e)$$

Compared with the case in Eq. (15), these scattering quantities have the same expression except that the sine function is replaced by the hyperbolic sine function. In a similar way, at the band edge,  $K_a \Lambda = m\pi$ , we have

$$T_N = \frac{1}{bcN^2 + 1}, \quad (18a)$$

$$R_{NL} = \frac{b^2}{bc + 1/N^2}, \quad R_{NR} = \frac{c^2}{bc + 1/N^2}, \quad (18b)$$

$$W_{NL} = \frac{bc - b^2}{bc + 1/N^2}, \quad W_{NR} = \frac{bc - c^2}{bc + 1/N^2}. \quad (18c)$$

So far we have derived the analytic solutions for the physical quantities  $T_N$ ,  $R_{NL}$ ,  $R_{NR}$ ,  $W_{NL}$ , and  $W_{NR}$  to measure the scattering, absorbing and radiating properties of 1DPTSPC.

### III. RESULT AND DISCUSSION

In this section, we disclose detailedly these optical properties of 1DPTSPC combing with its band structure. Figure 2 illustrate the real band structure, the complex band structure and the corresponding optical properties in the absence of gain and loss  $\varepsilon'' = 0$ , which is already studied very well. Here in the conduction band regions these two band structures coincide with each other very well, but in the band gap regions, for the real band structure the wave vector becomes complex, in the following discussions we will disclose that as  $\varepsilon''$  is increased in the conduction band regions the eigenfrequency may become complex. We emphasize that the one dimensional photonic crystal here is also T-symmetric, and so  $b = c$ ,  $R_{NL} = R_{NR} \geq 0$  and  $W_{NL} = W_{NR} = 0$  derived from Eqs. (15) and (17). For every conduction band,  $K\Lambda$  varies between 0 and  $\pi$ , there are  $N - 1 = 9$  points where transmission resonances occur, because when  $K\Lambda = \frac{n\pi}{N}$  ( $n = 1, 2, \dots, N - 1$ ),  $\sin NK\Lambda / \sin K\Lambda = 0$ , so  $T_N = 1$  can be obtained from Eq. (15a). At the same frequencies, the reflectances from both sides are zero  $R_{NL} = R_{NR} = 0$  which can be seen from Eqs. (15b) and (15c). In the band

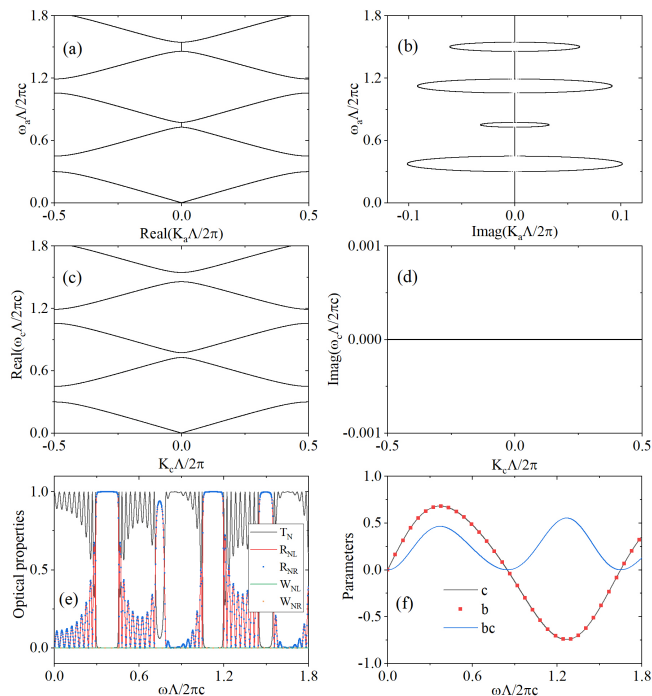


Figure 2. (Color online) Real band structure (a), (b) and complex band structure (c), (d) of the 1DPTSPC in the absence of gain and loss  $\varepsilon''=0.0$ . (e) The optical properties  $T_N$ ,  $R_{NL}$ ,  $R_{NR}$ ,  $W_{NL}$  and  $W_{NR}$  as function of the reduced frequency in the absence of gain and loss. (f) The values of the parameters  $c$ ,  $b$  and  $bc$  as function of the reduced frequency.

gap,  $\sinh^2 NK_{ai}\Lambda / \sinh^2 K_{ai}\Lambda$  is much larger than one, so  $T_N = 0$  can be derived from Eq. (17a), moreover,  $R_{NL} = R_{NR} = 1$  can be obtained from Eqs. (17b) and (17c).

In Fig. 3, we present the complex band structures for different values of the imaginary relative permittivity  $\varepsilon''$  through the method proposed in Ref. [28]. In our calculation, 16 lowest bands in the absence of gain and loss are considered to expand the Bloch waves in the corresponding  $\mathcal{PT}$ -symmetric photonic crystal. As  $\varepsilon''$  is increased from zero, the eigenfrequency for all the band stay real for small value of  $\varepsilon''$  as shown in Figs. 3(a) and 3(b), when  $\varepsilon''$  is increased to some critical value, the first band gap start to vanish and the first and second bands begin to coalesce, then exceptional point emerges at the center of the Brillouin zone as shown in Figs. 3(c) and 3(d). As  $\varepsilon''$  is increased further, these exceptional points move and the complex eigenfrequencies which are conjugate to each other emerge, this property agrees with non-Hermitian quantum mechanics, the band region with complex eigenvalue form the  $\mathcal{PT}$ -broken phase, otherwise the band region with real eigenvalue form the  $\mathcal{PT}$ -exact phase. As  $\varepsilon''$  continues to be increased, the exceptional points which originates from the coalescence of the third and fourth band emerges at the edge of Brillouin zone, then the corresponding  $\mathcal{PT}$ -broken phase expands, these can be seen from Figs. 3(e) and 3(f). If we further increase  $\varepsilon''$  from

1.0, the second band gap reopens, and the  $\mathcal{PT}$ -broken phase, which originates from the coalescence of the second and third band expands, emerges at the Brillouin center and evolves into a band where the eigenvalues are all conjugate complex numbers for all Bloch wave vectors. The  $\mathcal{PT}$ -broken phase which originates from the coalescence of the third and fourth band also expands, emerges at the edge of Brillouin zone, stop to expand at some critical value of  $\varepsilon''$ , then this  $\mathcal{PT}$ -broken phase is decreased, and evolve into a complete real band. These phenomena can be seen from Figs. 3(g), 3(h), 3(i) and 3(j). Some of these preceding discussions are disclosed in the Ref. [28], but we further point out the behaviours of the complex bands after  $\varepsilon''$  is increased from 1.0.

Through the complex band structure we can distinguish the  $\mathcal{PT}$ -exact and  $\mathcal{PT}$ -broken phases easily, however, the frequency in the study on the optical properties is taken to be real, so we can also depict the corresponding real band structure which are shown in the Appendix A. In fact, the part of the complex band structure with real eigenfrequency coincides with the part of the real band structure with real Bloch wave vector. We can identify the band gap from the complex band structure, which locates at the gap between the real parts of two adjacent bands.

Figure 4 shows the transmittance, reflectances and the parameters ( $b$ ,  $c$  and  $bc$ ) from both sides at the different values of  $\varepsilon''$ , here the number of unit cells is chosen to be  $N = 10$ . The values of the optical properties ( $T_N$ ,  $R_{NL}$ ,  $R_{NR}$ ,  $W_{NL}$  and  $W_{NR}$ ) we study here are denoted by  $\rho$ , it is very large at some frequencies, in order to observe their variation we take the ordinate as  $y = \frac{4}{\pi} \tan^{-1} \rho$ , in this scale, if  $\rho = 1$ ,  $y = 1$ , and if  $\rho$  approach  $\pm\infty$ ,  $y$  approach  $\pm 2$ . Combined with Fig. 3 and 4, it can be easily seen that these properties are closely related to the band structure. For some conduction bands of which all the eigenstates in the band structure are in the  $\mathcal{PT}$ -exact phase,  $K\Lambda$  varies from 0 to  $\pi$ , in addition to the premise that  $b$  and  $c$  are finite, there are  $N - 1 = 9$  points where transmission resonances occurs, at the same frequencies,  $R_{NL} = R_{NR} = 0$  and  $W_{NL} = W_{NR} = 0$  which can be seen from Eqs. (15b)-(15e) for the same reason in Fig. 2. The difference is that for nonzero  $\varepsilon''$ , a part of a complex conduction band with real frequency may be not complete, that is to say,  $K\Lambda$  varies in a part of the section  $[0, \pi]$ , consequently, in this band region there are less than  $N - 1 = 9$  points corresponding to the transmission resonances. In the band gap, the transmittance is zero  $T_N = 0$ , one of  $R_{NL}$  and  $R_{NR}$  is greater than one and the other is less than one, which can be derived from the generalized conservation law, in this case  $\sqrt{R_L R_R} = 1$ .

As can be seen from Fig. 3 and Fig. 4, when the exceptional point emerges, near this position,  $bc$  becomes negative, so the transmittance  $T_N$  is larger than one which can be derived from Eq. (15a), moreover, if  $\sin^2 NK\Lambda / \sin^2 K\Lambda$  approach  $|1/bc|$  in some cases, the transmittance  $T_N$  can arrive at a very large value, and out of the generalized conservation law one of  $R_{NL}$  and

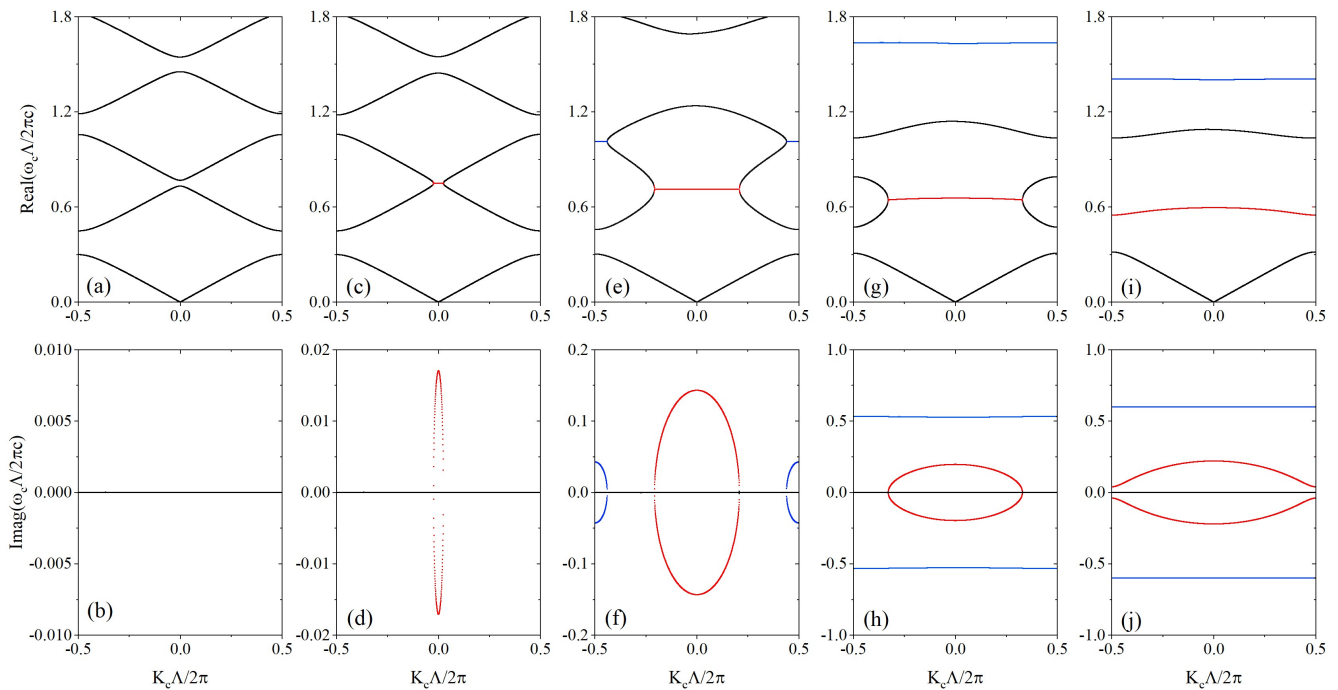


Figure 3. (Color online) Complex band structures of the 1DPTSPC at  $\varepsilon''=0.1$  (a) and (b),  $\varepsilon''=0.2$  (c) and (d),  $\varepsilon''=1.0$  (e) and (f),  $\varepsilon''=1.5$  (g) and (h),  $\varepsilon''=2.0$  (i) and (j). The top five graphs show the real parts of the complex eigenfrequencies, and the bottom five graphs denote the corresponding imaginary parts of the complex eigenfrequencies.

$R_{NR}$  or both of them will reach large values. For example,  $T_N$  reaches 689.35,  $R_{NL}$  and  $R_{NR}$  reach 8804.24 and 53.82 at the same time when  $\varepsilon'' = 0.2$  shown in Fig. 4(c). However, in other conduction band regions and all the band gaps,  $T_N$ ,  $R_{NL}$  and  $R_{NR}$  can't reach large values at the same time, because in these regions,  $bc$  is great than zero, so  $T_N$  can't be great than 1 as a result of Eq.(15a). The scattering properties at the second band when  $\varepsilon'' = 2.0$  seem to violate this statement, we can see in Fig. 4(i), at the frequency 0.545,  $T_N = 13.79$ ,  $R_{NL} = 1.2 \times 10^4$  and  $R_{NR} = 1.35 \times 10^{-2}$ , actually, it does not violate this statement, because there is an exceptional point near this frequency, it isn't shown in the complex band structure because the computational method we use here is approximate, while it can be shown in the real band structure in Appendix A which is obtained by a more accurate method.

In the band gap, as  $\varepsilon''$  is increased from 0 to 2.0, the gap between  $R_{NL}$  and  $R_{NR}$  becomes very large. When  $\varepsilon''$  is greater than 0.5, we can see  $R_{NL}$  is very large and  $R_{NR}$  is very small. We call this phenomenon unidirectional weak visibility, there are some similarities and differences between this phenomenon with the unidirectional invisibility. The reflectance from one side in the phenomenon of unidirectional invisibility is zero, but in our phenomenon the corresponding reflectance from one side is very small and not zero, the reflectance from the other side in these two phenomena are both very large, and the corresponding reflectance in our phenomenon seems to be even larger. More than that, the transmittance is 1 in

the unidirectional invisibility, while the transmittance in our phenomenon is 0 which occurs in the band gap, this is the significant difference that is different from the unidirectional invisibility. For example,  $R_{NL}$  is more than 9.28 and  $R_{NR}$  is less than 0.108 in the second band gap ( $1.245 < \text{reduced frequency} < 1.7$ ) at  $\varepsilon'' = 1.0$ ,  $R_{NL}$  is more than 7.5 and  $R_{NR}$  is less than 0.133 in the second band gap ( $1.16 < \text{reduced frequency} < 1.89$ ) at  $\varepsilon'' = 1.5$ . The unidirectional weak visibility in the band gap can possess wide frequency range.

It can be also seen from Fig. 3 that as  $\varepsilon''$  is increased the flat bands with narrow frequency range emerges, some of them are real band, for example as  $\varepsilon''$  increases from 1.5, the second complete real band becomes flat band and narrower and narrower. In Fig. 4 we can see obvious resonances [33] in this region. At both sides of this band, there are two large band gaps, by taking advantage of this property the  $\mathcal{PT}$ -symmetric photonic crystal can be used as filter [34], only the wave with frequency located in this narrow range can transmit through it.

In addition to the study on the scattering properties, we also plot the absorptances with incidence from the left and right sides in Fig. 5(a) and 5(b) when  $\varepsilon'' = 0.2$  and  $\varepsilon'' = 1.0$ , respectively. It can be seen from Fig. 5(a) that near the exceptional point  $bc$  is negative,  $W_L$  can arrive at -9492.6 and  $W_R$  can reach -742.2 at the same time, that means the optical effect of the 1DPTSPC is amplifying from both sides. For the first band gap, the lines of  $W_{NL}$  and  $W_{NR}$  cross each other shown in Fig. 5(a) and 5(b), actually this phenomenon also happens for all  $\varepsilon''$

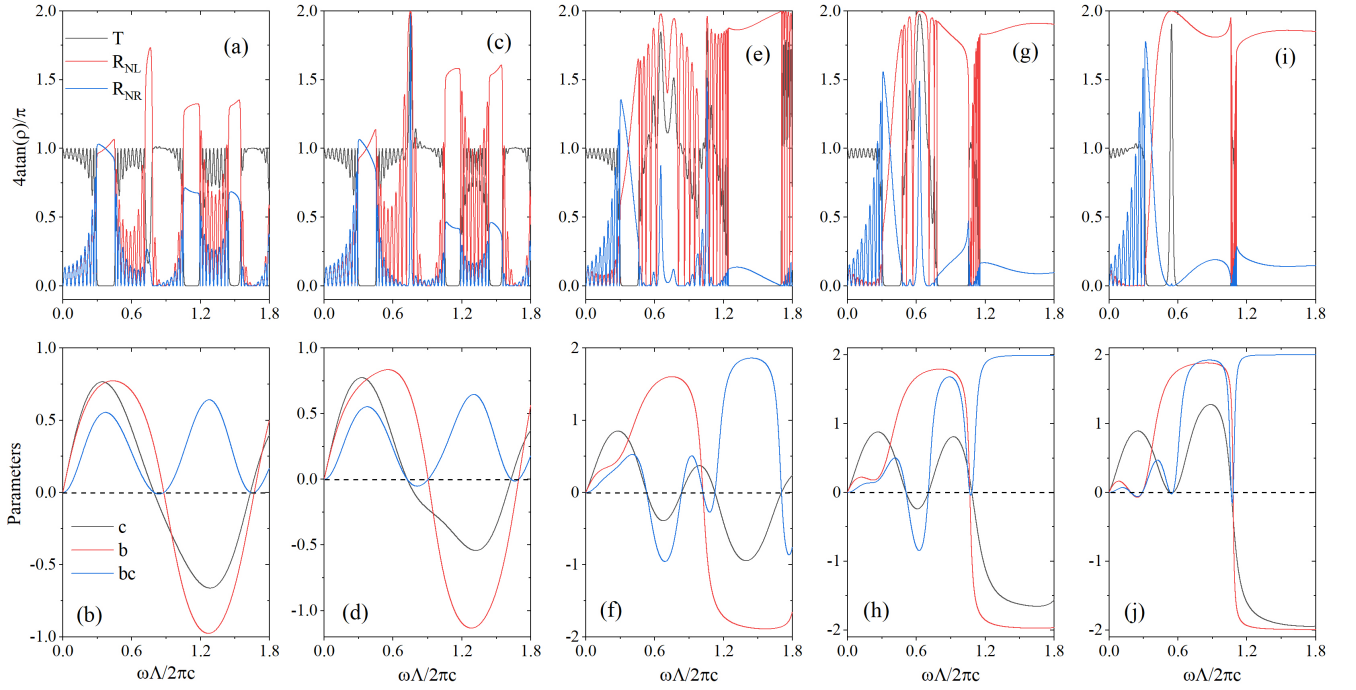


Figure 4. (Color online) Transmittance ( $T_N$ ) and reflectances ( $R_{NL}$  and  $R_{NR}$ ) of the 1DPTSPC with  $N=10$  periods at  $\varepsilon''=0.1$  (a) and (b),  $\varepsilon''=0.2$  (c) and (d),  $\varepsilon''=1.0$  (e) and (f),  $\varepsilon''=1.5$  (g) and (h),  $\varepsilon''=2.0$  (i) and (j).  $T_N$ ,  $R_{NL}$  and  $R_{NR}$  are denoted by the black, red and blue lines in the top five panels,  $c$ ,  $b$  and  $bc$  are marked by the black, red and blue lines in the bottom five panels.

we consider in the text. This can be also illustrated by using Eqs. (17d) and (17e),  $bc$  is larger than zero in this region, and  $b$  isn't equal to  $c$  in general, the denominators of  $W_{NL}$  and  $W_{NR}$  are equal to each other, one of their numerators is more than zero, then the other is less than zero, so  $W_{NL}$  and  $W_{NR}$  have different signs. At the cross point where  $W_{NL}$  and  $W_{NR}$  take the same value, it can be easily seen from Eqs. (17d) and (17e) that only when  $b = c$ ,  $W_{NL} = W_{NR}$  and they are both equal to zero. In general, when  $bc$  is larger than zero, these two absorptances have opposite signs, while  $bc$  is less than zero, these two absorptances can be both negative.

We also investigate the field intensity distribution in the 1DPTSPC when the light is incident from the left and right sides. In Fig. 5(c) and 5(d), we plot the field intensity distribution when the reduced frequency is chosen at the point near exceptional point for  $\varepsilon'' = 0.2$ , it can be seen that when the light is incident from the left side the field intensity decays along the propagation direction and when the light is incident from the right side the field intensity grows along the propagation direction. The field intensity distribution when the reduced frequency is fixed at the band gap is also considered in Fig. 5(e) and 5(f), we find that the field intensity decays sharply along the propagation direction when the light is incident from the both sides in the band gap, so that the logarithmic coordinate is used to denote the variation. These phenomena agree with our preceding discussions.

#### IV. CONCLUSION

We have defined the generalized absorptance to include the amplifying effect of the active dielectric, derived the mathematical expressions of the optical properties of 1DPTSPC, and expounded and analyzed these optical properties. Combing with the band structure, we find that some singular behaviors appear near the exceptional points, the transmittance and reflectances from both sides are greater than one and even all reach large values at the same time, and then the corresponding absorptances from both sides are negative. In the band gap, we find the phenomenon of unidirectional weak visibility, the transmittance is zero, the reflectance from one side is very large, while the reflectance from the other side is very small. Based on this study, we envision various applications in the designs of the optical functional devices.

#### ACKNOWLEDGMENTS

This work is supported by the National Natural Science Foundation of China (Grant No. 12004231), the Science and Technology Innovation Planning Project in Universities and Colleges of Shanxi Province of China (Grant No. 2019L0019), and the Applied Basic Research Program of Shanxi Province of China Grant (No. 201901D211165).

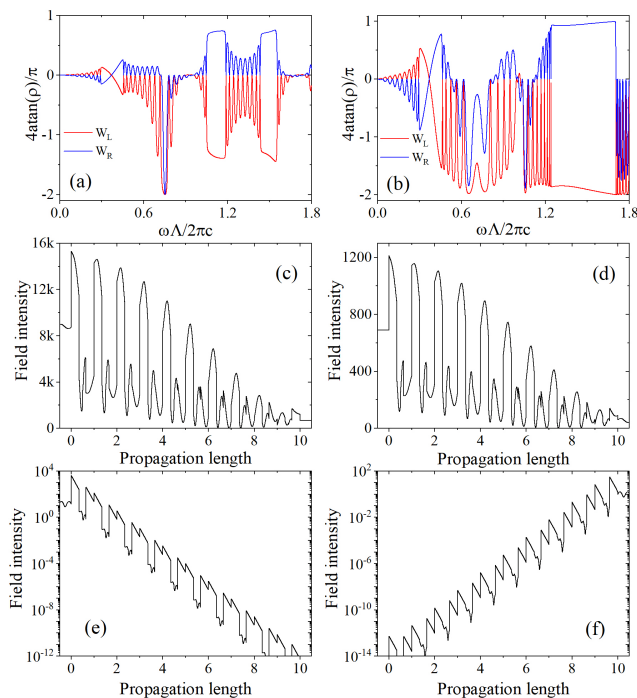


Figure 5. (Color online) Absorptance spectra ( $W_{NL}$  and  $W_{NR}$ ) of the 1DPTSPC with  $N=10$  periods at  $\varepsilon''=0.2$  (a) and  $\varepsilon''=1.0$  (b). Field intensity distribution inside the  $\mathcal{PT}$ -symmetric photonic crystal for incidence from the left side ((c) and (e)) and right side ((d) and (e)). The reduced frequency  $\omega\Lambda/2\pi c=0.75352$  and  $\varepsilon''=0.2$  are chosen for the panels (c) and (d),  $\omega\Lambda/2\pi c=1.5$  and  $\varepsilon''=1.0$  are fixed for the panels (e) and (f), respectively.

### Appendix A: Optical properties of 1DPTSPC at higher frequency

In Fig. 6 we present the real band structure corresponding to the complex band structure in Fig. 3 in the main text. After comparing these figures we find that the part of the complex band structure with real eigenfrequency coincides with the part of the real band structure with real Bloch wave vector, the parts with complex Bloch wave vector correspond to the band gaps. When  $\varepsilon'' = 2.0$ , it can be seen from Fig. 6(i) and 6(j) that there are some parts of the conduction band structure with real Bloch wave vector near the reduced frequency 0.56, but this isn't demonstrated in the Fig. 3(i) and 3(j), so the sharp transmittance in Fig. 4(i) near the reduced

frequency 0.56 can be explained.

We also consider the cases if  $\varepsilon''$  continues to be increased from 2.0. Figure 7 shows the evolution of the band structures when the values of  $\varepsilon''$  are chosen at 4.0, 6.5, 7.0, 8.0 and 12.0, respectively. In the Fig. 7(a) the first complex band starts to move down and intersects with the first real band, the eigenfrequencies at two cross points turn to be real as  $\varepsilon''$  is increased to a critical value in Figs. 7(c) and 7(d), then these two bands start to coalesce, the two cross points are exceptional points. As  $\varepsilon''$  is increased further, as shown in Figs. 7(e)-7(h), each exceptional point splits two, the middle part belong to real band, the first real band start to coalesce with the second real band, the exceptional points are generated at the edge of Brillouin zone and move to the center of Brillouin zone, in this progress, the second real band disappears and a complex band is generated. As can be seen from Figs. 7(g)-7(j), as  $\varepsilon''$  is increased, all the high bands are in the  $\mathcal{PT}$ -broken phase, only the circle part of band with low eigenfrequency is in the  $\mathcal{PT}$ -exact phase, moreover, this region decreases gradually with the increase of  $\varepsilon''$ , disappears when  $\varepsilon''$  is increased continuously to a critical value, meanwhile, the only two exceptional points move to the center of Brillouin zone and then merge at this position, so all the bands belong to the  $\mathcal{PT}$ -broken phase. The corresponding real band structure is presented in Figure 8, the consistency can be also easily seen for these two band structures.

The corresponding optical properties transmittance, reflectances and the parameters ( $b$ ,  $c$  and  $bc$ ) are presented in Fig. 9 at different values of  $\varepsilon''$ , here the number of unit cells is also fixed at  $N = 10$ . These values may be also very large, so we also take the ordinate as  $y = \frac{4}{\pi} \tan^{-1} \rho$ . We also find similar phenomena exhibited in the main text, if the frequency of the incident light is near the exceptional point, here the word near means that the frequency or  $\varepsilon''$  is taken near the corresponding values of the exceptional point, the transmittance, and reflectances may be much larger than one at the same time, if the frequency or  $\varepsilon''$  is located at the other region, then  $T_N$ ,  $R_{NL}$  and  $R_{NR}$  can't reach large values at the same time. Moreover, we also see the perfect resonances at the almost perfect flat bands, for example, it can be seen from Fig. 9(a) and 9(c) that the resonances exhibit when the reduced frequencies are 0.95 and 0.66, respectively. The absolute values of  $b$  and  $c$  at the band gap become larger and larger as  $\varepsilon''$  is increased.

[1] R. El-Ganainy, K. G. Makris, M. Khajavikhan, Z. H. Musslimani, S. Rotter, and D. N. Christodoulides, *Nat. Phys.* **14**, 11 (2018).  
[2] N. Moiseyev, *Non-Hermitian Quantum Mechanics* (Cambridge University Press, 2011).  
[3] C. M. Bender and S. Boettcher, *Phys. Rev. Lett.* **80**, 5243 (1998).

[4] C. M. Bender, D. C. Brody, and H. F. Jones, *Phys. Rev. Lett.* **89**, 270401 (2002).  
[5] C. M. Bender, S. Boettcher, and P. N. Meisinger, *J. Math. Phys.* **40**, 2201 (1998).  
[6] M. A. Miri and A. Alù, *Science* **363**, eaar7709 (2019).  
[7] H. Ramezani, T. Kottos, V. Kovanic, and D. N. Christodoulides, *Phys. Rev. A* **85**, 153 (2012).

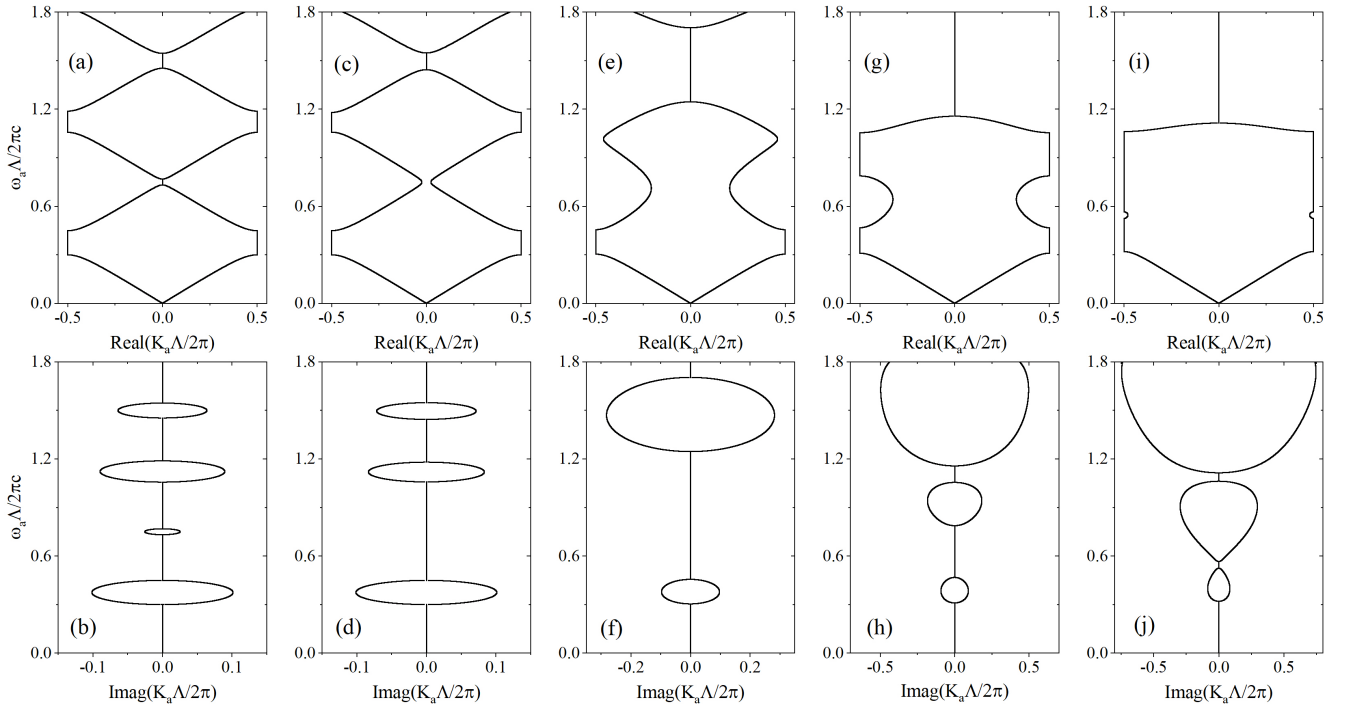


Figure 6. Real band structures of the 1DPTSPC at  $\epsilon''=0.1$  (a) and (b),  $\epsilon''=0.2$  (c) and (d),  $\epsilon''=1.0$  (e) and (f),  $\epsilon''=1.5$  (g) and (h),  $\epsilon''=2.0$  (i) and (j). The top five graphs show the real parts of the Bloch wave vectors, and the bottom five graphs denote the corresponding imaginary parts of the Bloch wave vectors.

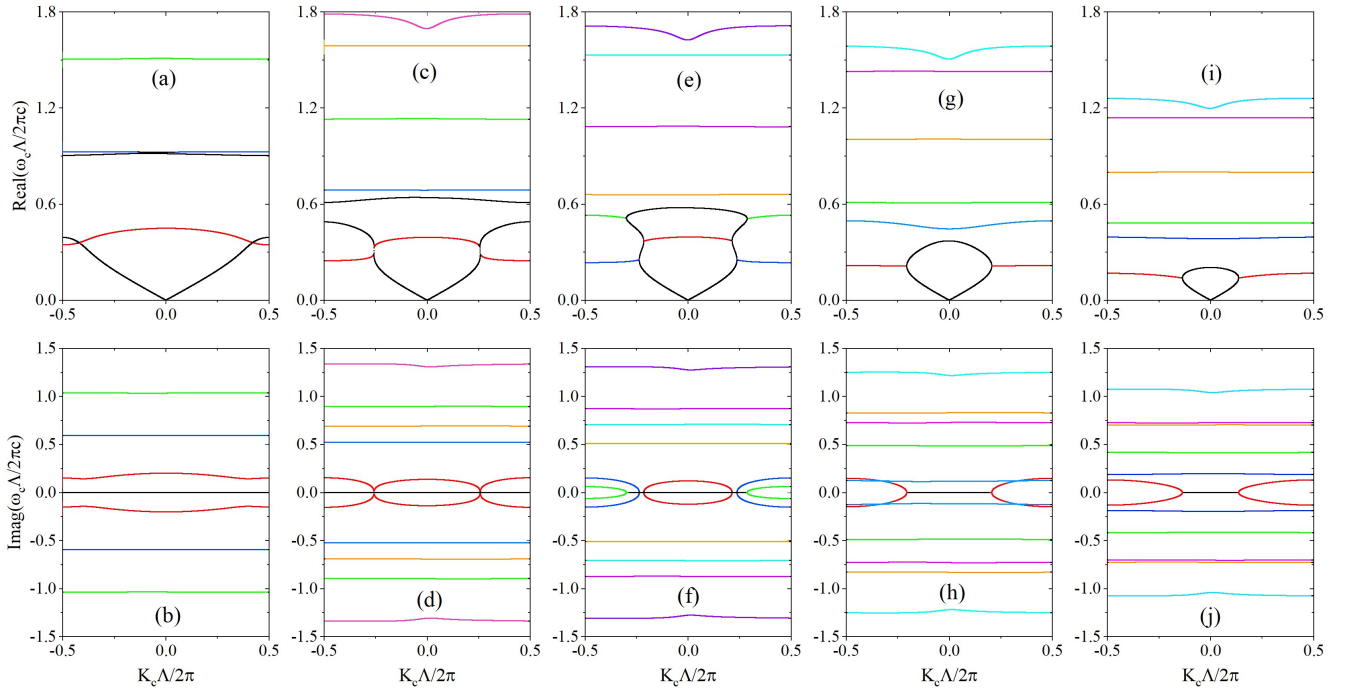


Figure 7. (Color online) Complex band structures of the 1DPTSPC at  $\epsilon''=4.0$  (a) and (b),  $\epsilon''=6.5$  (c) and (d),  $\epsilon''=7.0$  (e) and (f),  $\epsilon''=8.0$  (g) and (h),  $\epsilon''=12.0$  (i) and (j). The top five graphs plot the real parts of the complex eigenfrequencies, and the bottom five graphs illustrate the corresponding imaginary parts of the complex eigenfrequencies. All the other parameters are identical to that in Fig. 2 in the main text.

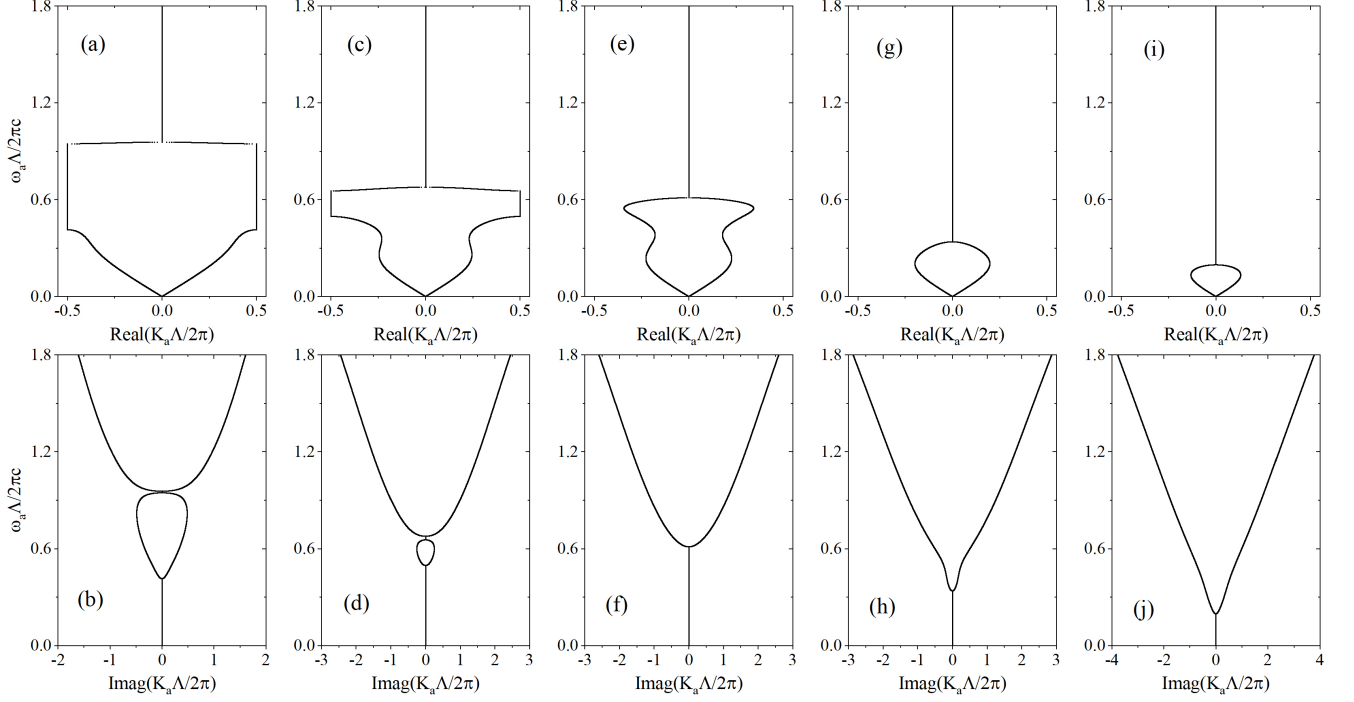


Figure 8. Real band structures of the 1DPTSPC at  $\epsilon''=4.0$  (a) and (b),  $\epsilon''=6.5$  (c) and (d),  $\epsilon''=7.0$  (e) and (f),  $\epsilon''=8.0$  (g) and (h),  $\epsilon''=12.0$  (i) and (j). The top five graphs exhibit the real parts of the Bloch wave vectors, and the bottom five graphs denote the corresponding imaginary parts of the Bloch wave vectors.

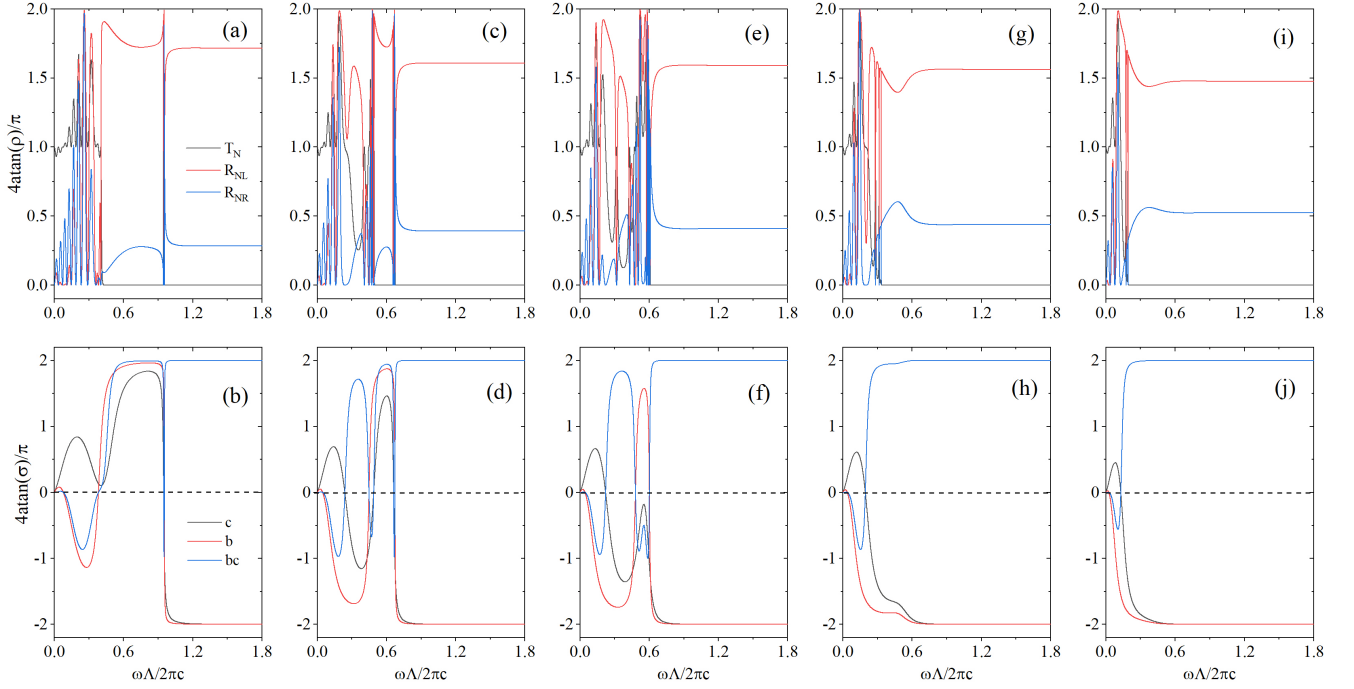


Figure 9. (Color online) Transmittance ( $T_N$ ) and reflectances ( $R_{NL}$  and  $R_{NR}$ ) of the one  $\mathcal{PT}$ -symmetric photonic crystal with  $N=10$  periods at  $\epsilon''=4.0$  (a) and (b),  $\epsilon''=6.5$  (c) and (d),  $\epsilon''=7.0$  (e) and (f),  $\epsilon''=8.0$  (g) and (h),  $\epsilon''=12.0$  (i) and (j).  $T_N$ ,  $R_{NL}$  and  $R_{NR}$  are denoted by the black, red and blue lines in the top five panels,  $c$ ,  $b$  and  $bc$  are marked by the black, red and blue lines in the bottom five panels.

- [8] Z. Xu-Lin and C. T. Chan, Phys. Rev. A **98**, 033810 (2018).
- [9] Y. X. Xiao, Z. Q. Zhang, Z. H. Hang, and C. T. Chan, Phys. Rev. B **99**, 241403 (2019).
- [10] W. D. Heiss, J. Phys. A **37**, 2455 (2003).
- [11] Z. Lin, H. Ramezani, T. Eichelkraut, T. Kottos, H. Cao, and D. N. Christodoulides, Phys. Rev. Lett. **106**, 213901 (2011).
- [12] V. A. Bushuev, D. M. Tsvetkov, V. V. Konotop, and B. I. Mantsyzov, Opt. Lett. **44**, 5667 (2019).
- [13] C. E. Rüter, K. G. Makris, R. El-Ganainy, D. N. Christodoulides, M. Segev, and D. Kip, Nat. Phys. **6**, 47 (2010).
- [14] L. Feng, Y. L. Xu, W. S. Fegadolli, M. H. Lu, J. E. B. Oliveira, V. R. Almeida, Y. F. Chen, and A. Scherer, Nat. Mater. **12**, 108 (2013).
- [15] X. F. Zhu, Y. G. Peng, and D. G. Zhao, Opt. Express **22**, 18401 (2014).
- [16] H. Ramezani, T. Kottos, R. El-Ganainy, and D. N. Christodoulides, Phys. Rev. A **82**, 043803 (2010).
- [17] S. Longhi, Phys. Rev. A **82**, 9583 (2010).
- [18] L. Feng, Z. J. Wong, R. Ma, Y. Wang, and X. Zhang, Science **346**, 972 (2014).
- [19] Z. J. Wong, Y. L. Xu, J. Kim, K. O'Brien, Y. Wang, L. Feng, and X. Zhang, Nat. Photonics **10**, 796 (2016).
- [20] H. Hodaei, M. A. Miri, M. Heinrich, D. N. Christodoulides, and M. Khajavikhan, Science **346**, 975 (2014).
- [21] Y. D. Chong, L. Ge, and A. D. Stone, Phys. Rev. Lett. **106**, 093902 (2011).
- [22] L. Ge and L. Feng, Phys. Rev. A **94**, 043836 (2016).
- [23] L. Ge, Y. D. Chong, and A. D. Stone, Phys. Rev. A **85**, 445 (2012).
- [24] A. Y. Song, Y. Shi, Q. Lin, and S. Fan, Phys. Rev. A **99**, 013824 (2019).
- [25] H. Alaeian and J. A. Dionne, Phys. Rev. B **89**, 188 (2014).
- [26] J. Schnabel, H. Cartarius, J. Main, G. Wunner, and W. D. Heiss, Phys. Rev. A **95**, 053868 (2017).
- [27] R. El-Ganainy, K. G. Makris, D. N. Christodoulides, and Z. H. Musslimani, Opt. Lett. **32**, 2632 (2007).
- [28] K. Ding, Z. Q. Zhang, and C. T. Chan, Coalescence of exceptional points and phase diagrams for one-dimensional pt-symmetric photonic crystals, Phys. Rev. B **92**, 235310 (2015).
- [29] Z. L. Zhen, F. Qin, Z. Qiang, and J. J. Xiao, Opt. Express **25**, 26689 (2017).
- [30] A. Cerjan, A. Raman, and S. Fan, Phys. Rev. Lett. **116**, 203902 (2016).
- [31] Y. Amnon and P. Yeh, *Optical waves in crystals: propagation and control of laser radiation* (New York City, NY: Wiley, 1984).
- [32] K. Sakoda, *Optical properties of photonic crystals* (Springer Science & Business Media, 2004).
- [33] S. Fan and J. D. Joannopoulos, Phys. Rev. B **65**, 235112 (2002).
- [34] S. Fan, P. Villeneuve, J. Joannopoulos, and H. Haus, Opt. Express **3**, 4 (1998).